



NEAR EAST UNIVERSITY
INSTITUTE OF GRADUATE STUDIES
DEPARTMENT OF MECHANICAL ENGINEERING

**DESIGN OF A TESTBENCH TO INVESTIGATE STABILITY IN THE PITCH OF A TILT-
WING UAV IN HOVER MODE**

M.Sc. THESIS

AHMED HAMID MOHAMED ABDALLA ZAKWAN

Nicosia

January, 2023

**AHMED HAMID MOHAMED
ABDALLA ZAKWAN**

**DESIGN OF A TESTBENCH TO INVESTIGATE STABILITY
IN THE PITCH OF A TILT-WING UAV IN HOVER MODE**

M.Sc. THESIS

2023

**NEAR EAST UNIVERSITY
INSTITUTE OF GRADUATE STUDIES
DEPARTMENT OF MECHANICAL ENGINEERING**

**DESIGN OF A TESTBENCH TO INVESTIGATE STABILITY IN THE PITCH OF A
TILT-WING UAV IN HOVER MODE**

MSc Thesis

AHMED HAMID MOHAMED ABDALLA ZAKWAN

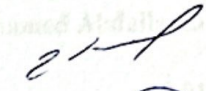
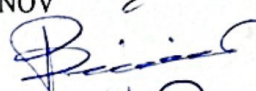
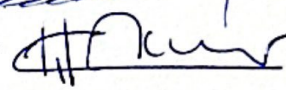
**Supervisor
Assoc.Prof. Dr. Huseyin CAMUR**

Nicosia

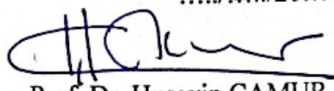
January, 2023

Approval


We certify that we have read the thesis submitted by Ahmed Hamid Mohamed Abdalla Zakwan titled **DESIGN OF A TESTBENCH TO INVESTIGATE STABILITY IN THE PITCH OF A TILT-WING UAV IN HOVER MODE** and that in our combined opinion it is fully adequate, in scope and in quality, as a thesis for the degree of Master of Sciences.

Examining Committee	Name-Surname	Signature
Head of the Committee:	Assist. Prof. Dr. Elbrus Basher IMANOV	
Committee Member*:	Assist. Prof. Dr. Metin BILIN	
Supervisor:	Assoc. Prof. Dr. Huseyin CAMUR	

Approved by the Head of the Department

08/02/20.23

Assoc. Prof. Dr. Huseyin CAMUR
Head of Department

Approved by the Institute of Graduate Studies


Prof. Dr. Kemal Hüsnü Can Başer
Head of the Institute

Declaration

I hereby declare that all information, documents, analysis and results in this thesis have been collected and presented according to the academic rules and ethical guidelines of Institute of Graduate Studies, Near East University. I also declare that as required by these rules and conduct, I have fully cited and referenced information and data that are not original to this study.

Ahmed Hamid Mohamed Abdalla Zakwan

10.01.2023

Acknowledgements

I would like to express my deepest gratitude to my supervisor, Assoc. Prof. Dr. Huseyin Camur, for his invaluable guidance, support and encouragement throughout the course of my research. His expertise and knowledge have been instrumental in the successful completion of this thesis.

I would also like to extend my appreciation to my mentor and friend, Dr. Pavel Makarov, for his invaluable support and encouragement throughout the research process. His knowledge and expertise have been an inspiration to me.

I am also grateful to my colleague Devan Rudolph for his support, encouragement, and helpful suggestions.

My family has been a constant source of love and support throughout my academic journey. I am deeply grateful to them for their unwavering support and encouragement.

Lastly, I would like to extend my gratitude to my colleagues at Near East University Robotics for their support and assistance throughout the research process

Ahmed Hamid Mohamed Abdalla Zakwan

Abstract

DESIGN OF A TESTBENCH TO INVESTIGATE STABILITY IN THE PITCH OF A TILT-WING UAV IN HOVER MODE

Zakwan, Ahmed Hamid Mohamed Abdalla

MSc, Department of Mechanical Engineering

January 2023, 65 pages

Drones also named Unmanned Aerial Vehicles (UAVs) are aircrafts without an onboard pilot. Their flight is either pre-defined or controlled by computers on the ground. They are useful for a number of reasons: among them being, for military purposes where they can be used as targets and decoys. They can also be used in surveillance such as in border patrol. Recently, they have even been used in farming, where the UAV is given a pre-defined flight and it sprays pesticides along that route. Following these trends, Near East University laboratory developed a tilt-wing UAV named LANNER to cater for these needs. Initial tests showed there was a need for an elaborate test-bench to improve on its pitch control. A test-bench is then designed to help in this regard and is the subject of this study. PID controller which is a universally accepted control algorithm used in industry for quite some time now is used as the control system. An analytical approach is used at first to get the equations for a P and PD controller and finally a comparison between the analytical and experimental data is carried out.

Keywords: Vertical Takeoff and Landing, Unmanned Aerial Vehicle, PID Controller

Summary

DESIGN OF A TESTBENCH TO INVESTIGATE STABILITY IN THE PITCH OF A TILT-WING UAV IN HOVER MODE

Zakwan, Ahmed Hamid Mohamed Abdalla
MSc, Department of Mechanical Engineering
January 2023, 65 pages

Keywords: Vertical Takeoff and Landing, Unmanned Aerial Vehicle, PID Controller

Table of Contents

Approval	1
Declaration	2
Acknowledgements	3
Abstract	4
Summary	5
Table of Contents	6
List of Tables	8
List of Figures	9
List of Abbreviations	11

CHAPTER I

Introduction	12
Research Problem	13
Significance of the Study	13
Limitations	13
Motivation	13
Problem Statement	14
Thesis Layout	14

CHAPTER II

Literature Review	15
-------------------------	----

CHAPTER III

Theory	21
Dynamics of the System	24
P- Controller with no Latency	26
P- Controller with Latency	28
PD- Controller	29

CHAPTER IV

Methodology	32
Components used in the UAV	34
Design of the Test bench	39
Delay Estimation	41

CHAPTER V

Results and Discussion	42
------------------------------	----

CHAPTER VI

Conclusion	47
REFERENCES	48
APPENDICES	51
Appendix A. MATLAB Code for the Comparison between Theory and Experimental Data For 0.5 P Coefficient.	51
Appendix B. MATLAB Code for the Comparison between Theory and Experimental Data For 0.6 P Coefficient.....	53
Appendix C. MATLAB Code for the Comparison between Theory and Experimental Data For 0.4 P Coefficient.....	55
Appendix D. Code for the PID.....	57
Appendix X. Turnitin Report	65

List of Tables

	Page
Table 2.1: Comparison of the UAV configurations.	16
Table 3.1: Relation between d and l	22
Table 3.2: Relation between the moment of inertia (J) and d .	24
Table 5.1: Comparison of the k_p values.	46

List of Figures

	Page
Figure 2.1. Timeline of previous machine learning-related studies for UAVs	18
Figure 2.2. Block diagram of process control using PID	19
Figure 3.1. Free body diagram of the system	21
Figure 3.2. Side view of the system	22
Figure 3.3. Front view of the system.	23
Figure 4.1. A right-side view of the fuselage with the battery holder.	32
Figure 4.2. A front view of the fuselage with the battery holder.	33
Figure 4.3. A top view of the fuselage.	33
Figure 4.4. Servo motor.	34
Figure 4.5. Example of an ESC.	34
Figure 4.6. An Inertial Measurement Unit (IMU).	35
Figure 4.7. Microcontroller.	35
Figure 4.8. 3V Voltage Regulator.	36
Figure 4.9. Radio Receiver.	37
Figure 4.10. Remote Controller.	38
Figure 4.11. PCB layout.	38
Figure 4.12. Right and front views of the test bench stand.	40
Figure 4.13. Fuselage mounted on the test bench stand.	40
Figure 5.1. Centre of gravity (I) against d.	42
Figure 5.2. Moment of inertia (J) against d.	43
Figure 5.3. Comparison between experimental and theoretical data for Kp value 0.4.	44

Figure 5.4. Comparison between experimental and theoretical data for K_p value 0.5. 45

Figure 5.5. Comparison between experimental and theoretical data for K_p value 0.6. 45

List of Abbreviations

VTOL:	Vertical Takeoff and Landing
UAV:	Unmanned Aerial Vehicle
PID:	Proportional Integral Derivative

CHAPTER I

Introduction

There has been a lot of development in the Unmanned Aerial Vehicle (UAV) sector in recent years. Autonomy in UAVs has been something that has been sorted out for years. With the involvement of not only the military sector but also the commercial sector development of UAVs has increased substantially. The role of UAVs is increasing with each passing day. This is mainly attributed to the fact that they can perform tasks that could be dangerous, monotonous, or expensive if a human pilot is involved. These roles include military operations (M. Ma'sum et al., 2013), where drones can be sent to target enemies that are miles away. Forest fire monitoring, surveillance, aerial photography, smart agriculture (D. Tsouros et al., 2019), product deliveries which include medical equipment and medicine delivery (C. Thiels et al., 2014), and infrastructure inspections. They have also recently included drone racing. These are all roles that require the UAV to be stable and easily controllable.

This study has been ongoing for 2 years and became a thesis in the year 2022. During this period, the Robotics Laboratory at Near East University has been developing a Tilt wing Vertical Take-off and Landing (VTOL) aircraft named LANNER. Extensive research has been carried out on UAVs and much has been learned in this time.

A number of factors were considered before deciding on the development of the tilt-wing UAV. One of those is that the tilt-wing UAV has the capability to hover and take off vertically. This was a major advantage as it allows the UAV to take off from anywhere and not just in places that have a long runway.

Tilt-wing UAVs have also benefitted from advances in avionics and electronics have also greatly contributed to their reduced sizes hence making them lighter (Kontogiannis and Ekaterinaris 2013). This directly influences their range. It also enables them to be more efficient and the overall quality of the UAVs increases.

Research Problem

With the advancement of technology, the complications that arise are increasing with each passing day. Tilt-wing VTOL UAVs have been developed and tested by different manufacturers and institutions. However, there has not been a lot of research into tilt-wing UAVs with only 2 motors on the wings. Most of the research into tilt wing UAVs has been with either 3 or more motors on the wing and the aircraft's tail. This is mainly due to the fact that it is considerably easier to control and stabilize such aircraft than those of only 2 motors.

VTOL UAVs can be controlled and guided in various ways as seen in literature and in practice. These methods differ in practice and the type of aircraft they are used. The tilt-wing UAV developed by Near East University Laboratory has considerably good control in roll. This is not the case when it comes to pitch. Hence the need to develop a test bench that will be used to experiment and test the UAV to improve its pitch control in vertical mode.

Significance of the Study

As aforementioned, UAVs have numerous advantages. This study will build up an approach and contribute to the problem of combining the advantages of a fixed-wing aircraft and a Rotary-wing aircraft by detailing how to establish control, particularly in the pitch of these aircraft. This study can then be used in the design of future tilt-wing UAVs.

From their numerous advantages, they are quite attractive options in the development of air taxis and reconnaissance drones.

Limitations

There has not been a lot of research and development into tilt-wing UAVs. This creates difficulty as it does not become easy to find material on this topic.

Motivation

The motivation of this thesis stems from the interest that the general world has had in unmanned aerial vehicles for a while now. Their numerous uses ranging from military missions to home goods delivery have encouraged researchers to start developing unmanned aerial vehicles.

Drones could also be used to expand scientific research. There are drones that are currently being used to map large areas and monitor what is happening in these environments. They can also be used to monitor rivers and check for flooding. They are also used in monitoring wildlife and protecting them from poachers.

All these uses and more encourage the use and research and development of drones.

Problem Statement

The challenges facing the aviation sector with regard to avionics and flight control are getting more sophisticated with each passing day. Development and modeling of a tilt-wing UAV in vertical flight has been investigated in recent times (Sanchez Rivera et al, 2020). However, there is still a lack of enough material on this subject.

Therefore, the main objective of the thesis is to design a test bench and investigate how stability performance in hover mode will depend on varying design parameter (d). This is the distance from the tilt-wing axis to the position of the battery.

Thesis Layout

In chapter 1, An introduction into unmanned aerial vehicles, project definition, significance of the study, limitations and motivation for the project.

In chapter 2, A more detailed discussion of unmanned aerial vehicles is presented, together with a deep dive in types of control systems and what is available in the market. A discussion on which is the most preferred method for this thesis is also mentioned.

In chapter 3, An analytical approach to the project is looked at, which forms a base for the experimental stage of the project.

In chapter 4, The methodology used in the experiment, electronic components and the setup of the experiment done in the project are all mentioned in this chapter.

In chapter 5, Results from the experiment are compared to the analytics done in this chapter together with their discussion.

In chapter 6, A conclusion and future scope for further research is discussed in this chapter.

CHAPTER II

Literature Review

In recent times there has been a lot of advancement in unmanned aerial vehicles. An area where autonomous systems development is growing rapidly is drone racing. In this niche, there is a lot of research and practical work being done. The systems not only have to be fast enough but also respond to the ever-changing environment and try to win (Wagter et al. 2021).

This interest in UAVs is due to the numerous advantages they have. Their ability to have a wide range of movement coupled with their precision and their ease of deplorability has made them a really attractive feature not just to the military but also to the commercial sector.

Unmanned Aerial Vehicles (UAVs) can be classified into conventional UAVs, multirotor UAVs, and hybrid UAVs (Sanchez Rivera et al. 2020). Conventional UAVs can take off using a normal runway. They require large areas where they can build up the thrust to take off. Multirotor on the other hand does not need a runway and they can just take off vertically. An example of a multi-rotor is the helicopter.

Hybrid-design UAVs combines the capabilities of the other two classifications of UAVs; conventional and multirotor (Centinsoy et al., 2012). Hence when needed they can take off and land vertically and can also utilize a runway should the need arise. They are also called Vertical Take-off and Landing (VTOL) aircraft.

These Hybrid UAVs can be further classified into tilt-rotor UAVs and tilt-wing UAVs. Tilt-rotor UAVs generally have the motors of the aircraft on the tip of the wings. These rotors are the ones that tilt to enable the aircraft to take off vertically. One of the main disadvantages of tilt-rotor aircraft is that they lose so much thrust power when taking off vertically. This is because the wings are horizontal to the motors. The wings in a tilt rotor do not tilt.





Tilt-wing UAVs normally have the whole wing tilting when taking off vertically. This is a huge advantage compared to the tilt rotors as they can utilize more of the thrust in taking off. The motors could be more than 2 as seen in previous designs of this kind of aircraft. The tilt wing aircraft with just 2 motors brings about a balancing issue. It becomes hard to control this aircraft

than one with 4 motors as the one with 4 motors can react to the torques induced by the other motors.

A tilt-wing aircraft can have both of the wings tilting together or wings tilting individually. This is normally up to the design of the aircraft and what the designers require.

Table 2.1

Comparison of the UAV Configurations (Erceg et al., 2017)

Types	Advantages	Disadvantages	Example
Fixed wing	Long range Endurance	Horizontal take-off, requiring substantial space or support Inferior maneuverability compared to VTOL (Vertical Take-Off and Landing)	
Tilt wing	Combination of fixed wing and VTOL advantages	Expensive Technology complex	
Unmanned Helicopter	VTOL Maneuverability High payloads possible	Expensive Comparably high maintenance requirements	
Multicopter	Inexpensive, Low weight Easy to launch	Limited payloads Susceptible to wind due to low weight	

Source: adapted from Heutger, 2014 and Kelek, 2015

The choice of whether to have a fixed-wing aircraft or a multi-rotor UAV is determined by the mission profile of the aircraft. If endurance and range is a huge factor, fixed-wing aircraft are highly advantageous. On the other hand, if vertical take-off and landing is a necessity for the mission profile, multi-rotor UAVs are more suited to the task.

There has been a number of companies and organizations venturing into the design of tiltrotors but not as much has been done into tilt wing aircraft. Their flight dynamics being more complex could be one of the reasons why they have not been developed as much.

There are a number of VTOL UAVs available in the literature and those that are manufactured. One of those is the NASA GL- 10 (W. J. Fredericks et al., 2015) which is a hybrid tilt-wing aircraft. It is also known as Greased lightning. It has eight electric motor-driven propellers located on the leading edge of the wings. It also has 2 more motors on its horizontal stabilizer. The availability of all these motors act as redundancy while also generating more thrust for the aircraft. It has two 6kW diesel engines that charge lithium-ion batteries. It also has an endurance of 2hrs in forward flight mode.

Another tilt-wing aircraft that was being developed is the Dual tilt-wing UAV by the German company DHL (S. Mohsan et al., 2022). The thrust in this Dual Tilt-wing UAV was generated by two motors on the leading edge of the wings but unfortunately, there is not much development in recent years on this UAV.

Airbus Vahana (T. Ha et al., 2019) was an electric propeller-driven aircraft developed by the giant aircraft manufacturing company, Airbus. The reason for its development was urban mobility. It was a tilt-wing aircraft with eight fans for tilt-wing. The tilt-wing configuration was found to be superior at longer ranges. It had a wingspan of 6.25m, an empty weight of 695kg, and a maximum takeoff weight of 815kg. The Vahana was self-piloted and had a recorded longest single flight duration of 19 minutes, 56 seconds which was a distance covered of 50km.

(Ozdemir et al, 2013) developed a UAV named the TURAC which was a vertical takeoff and landing aircraft. They were able to design a fully electric aircraft that had 2 motors in the front and a ducted fan on the tail. It was able to successfully undergo tests.

KARI (Korean Aerospace Research Institute) has been able to develop several hybrid aircraft. Among them is the TR-90 which is a tilt-rotor UAV with a length of 3 meters, maximum speed of 250km/hr, a maximum takeoff weight of 210kg, and endurance of 5 hours.

Another one of their aircraft is the eVTOL (Electric Vertical Takeoff and Landing) OPPAV. It is an optionally piloted personal aerial vehicle with a length of 6.15 meters. It has a cruise speed of more than 200km/hr, a maximum takeoff weight of 650kgs, and a range of 50km.

The Quad Tilt Wing (QTW) VTOL UAV is another example of a tandem tilt wing aircraft. It has propellers mounted at the leading edge of each wing. It was developed to broaden civil UAV operations by the Japan Aerospace Exploration Agency (JAXA) (Muraoka et al 2012).

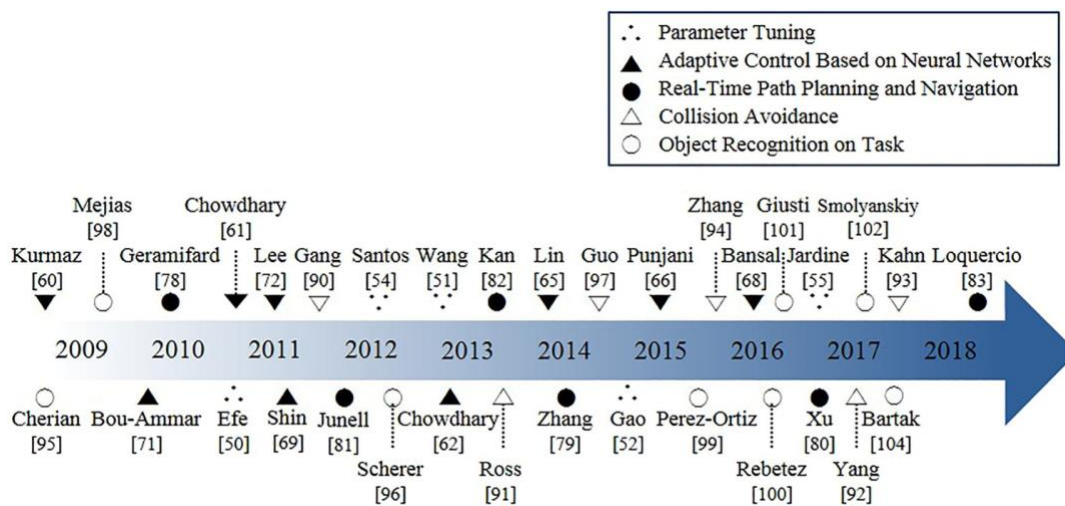
The V-22 Osprey (N. T. Hegde et al., 2019) is one of the most famous and successful hybrid UAVs. It is a tiltrotor UAV that is currently in use by the US military.

VTOL UAVs normally have four stages. These include take-off, transition, cruising, and landing. The control systems in these different modes could be different depending on the design of the aircraft.

Below is a figure showing the timeline of previous machine learning-related studies for UAVs.

Figure 2.1

Timeline of Previous Machine Learning-Related Studies for UAVs (Choi et al 2019)



There are several control systems used by UAVs in literature and the industry. A controller normally takes the error signal and converts it to a command. PID controllers are versatile controllers that use the present error, past error, and a prediction of the future error to calculate the appropriate actuator commands. PID stands for Proportional, Integral, and Derivative. The proportional, integral and derivative terms generally refer to how the error term is handled.

They can be used as just a P (Proportional) controller, PD (Proportional Derivative) controller, PI (Proportional Integral), or PID (Proportional Integral Derivative) controller.

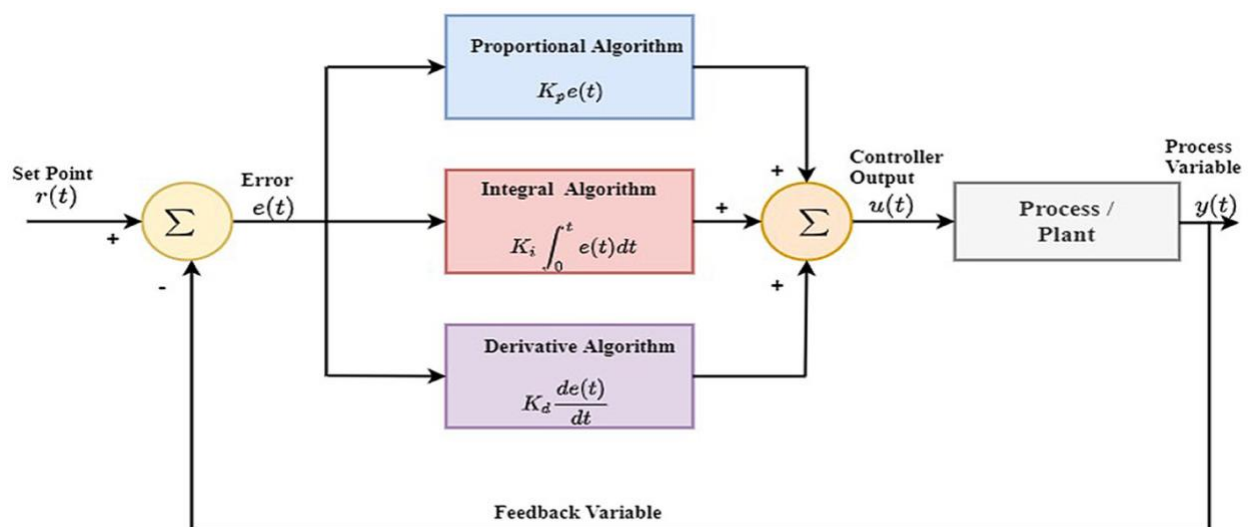
A PID controller essentially should be simple. This is mainly because it becomes easy to implement, easy to test and troubleshoot, and easy to understand.

The PID control algorithm can be described using the equation below:

$$u(t) = K_p e(t) + K_i \int_0^t e(\tau) d\tau + K_d \frac{d}{dt} e(t) \quad (2.1)$$

Figure 2.2

Block Diagram of Process Control Using PID (R. Borase et al., 2021)



The proportional controller takes the error and multiplies it by a proportional gain (K_p). The integral term takes the summation of the error and multiplies it by a constant (K_i). The derivative term takes the rate of change in error and multiplies it by a constant (K_d)

PID Controllers were introduced in the 1930s and they have been an industry standard since then. This is due to a number of reasons, among them being: they are simple, efficient and they are effective.

The paper by (E. Small et al, 2016) highlights a tilt-wing UAV's design and structural properties. It further elaborates on the mathematical modeling and how by using a cascaded P-PI and PID-based control system for the hover mode of the tilt-wing UAV, the UAV could hover in a stable mode. Their research also brought to light that having P-PI controller was indeed suitable as the responses were faster than having the cascaded PID. They were able to achieve this by taking into consideration a number of factors. Among them is having a design with as few moving parts as possible. This was mainly to reduce friction and it also acted as a way of making a structurally rigid and stable UAV. The tilt-wing UAV used in their research had two motors on the wings and one ducted fan on the tail.

Atheer L. Salih et al., (2010) researched the behavior of a quadrotor. They modeled a PID controller for the control of this quadrotor. The motors in the quadrotor act independently from the other motors. They are able to provide pitch, roll, and yaw control of the quadrotor. Diagonally opposite motors normally rotate in the same direction, while the other motors rotate in the opposite direction to these initial motors. Forward movement is provided by increasing the speed of the back motors and decreasing the speed of the front motors. The reverse also holds true. By using a mode-based controller which has independent controllers for each state, they were able to model a PID controller and by the use of the Ziegler Nichols method of tuning, the researchers were able to control the quadrotor and make sure they observed a stable reaction.

CHAPTER III

Theory

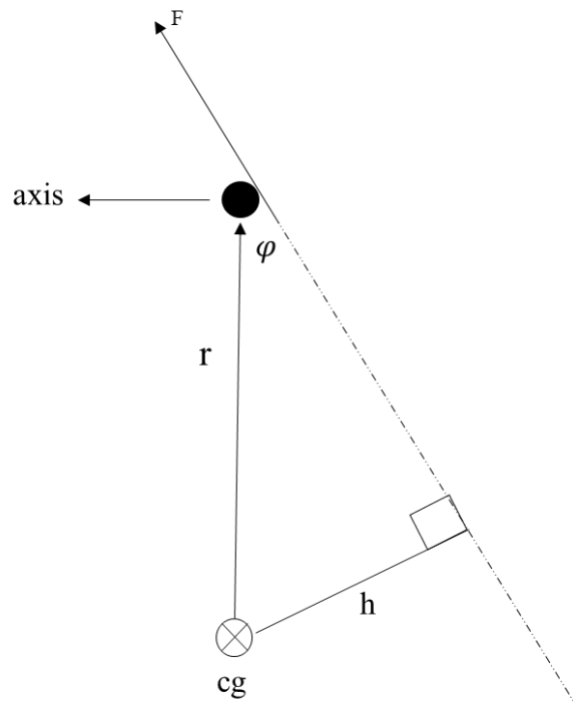
This thesis aims to investigate how stability performance in the hover mode of a tilt-wing UAV depends on the distance between the battery and the center of gravity and briefly explain how this affects the transition mode.

During the early stages of any experiment, theoretical values are based on the center of gravity and moment of inertia of the system (Roman Gabl et al, 2021).

For this to be achieved, we have to first look at the position of the battery as a function of the center of gravity of the whole system.

Figure 3.1

Free Body Diagram Of the System



The Center of gravity is an imaginary point where the body's total mass acts.

l is the distance between the position of the battery to the tilt-wing axis.

d is the distance between the system's center of gravity to the tilt-wing axis.

Figure 3.2

Side View of the System

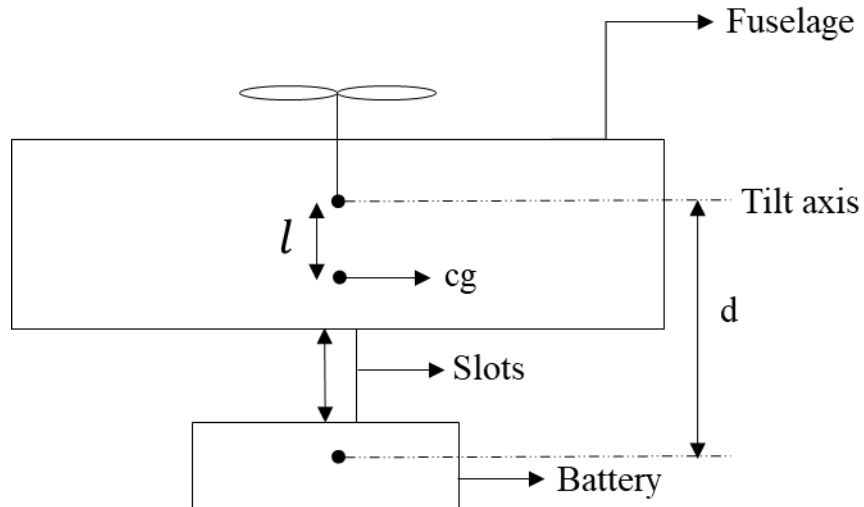


Table 3.1

Relation Between d and l

d	l
129.57mm	40.45mm
139.57mm	43.06mm
149.57mm	45.65mm
159.57mm	48.25mm

The data shown above is obtained from SOLIDWORKS.

It can be seen that the center of gravity is directly proportionally with the change in l . There is a linear relationship between the two.

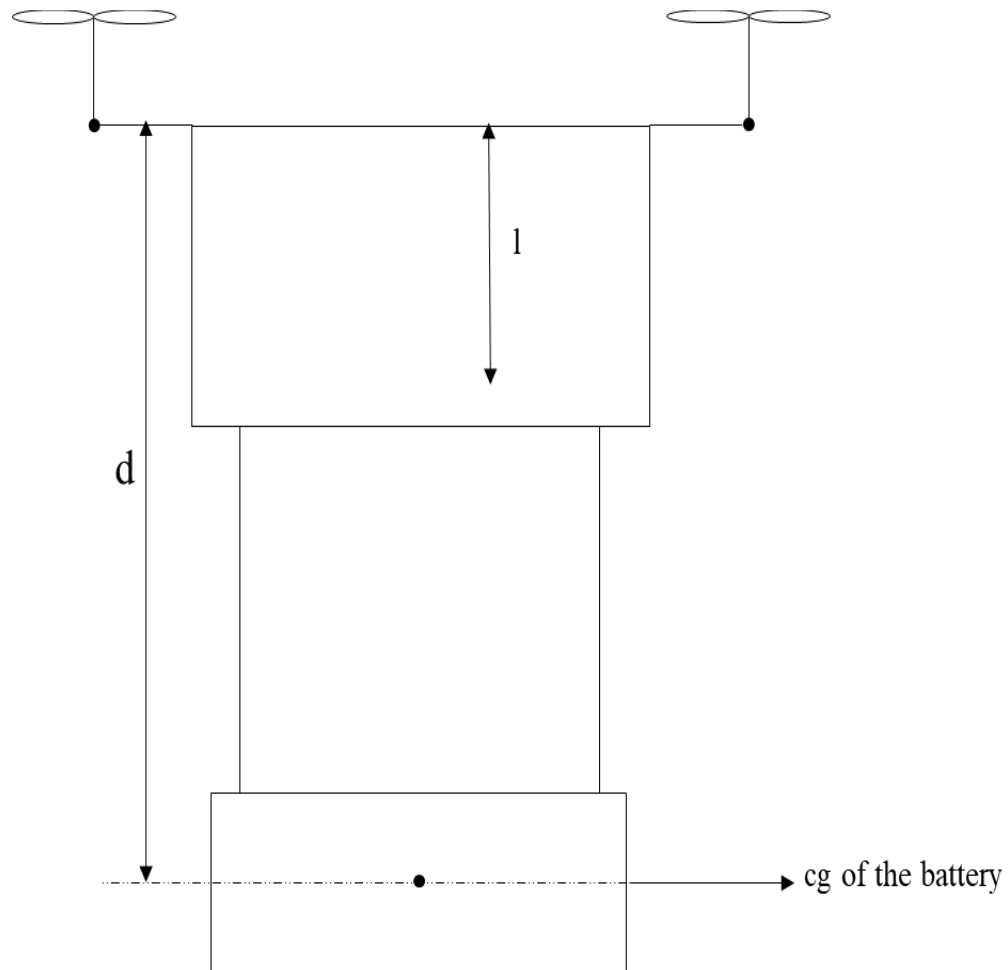
$$l = 0.2599 (d) + 6.7788 \quad (3.1)$$

Determining the moment of inertia of a body is crucial when it comes to aircraft design and control. Moment of inertia can be defined as a body's tendency to resist angular acceleration, which is the sum of the products of the mass of each particle in the body with the square of its distance from the axis of rotation.

There are several methods to measure the moment of inertia; physical pendulums, bifilar pendulums, compound pendulums, torsional pendulums, and torque (Or D. Dantsker et al, 2018). In this study, SOLIDWORKS which is a CAD software is used to determine the moment of inertia of the system.

Figure 3.3

Front View of the System



The moment of inertia of the system taken at the cg is found to be linearly related to the distance between the cg and the tilt wing axis. This is however not in match with the theory. In the formula for moment of inertia, it can be seen that the relation should be quadratic. The reason why it might be seen as linear could be because the battery is not heavy enough compared to the

rest of the fuselage. If we are to consider it as two parts, dynamic and static, with the battery as the moving part.

Table 3.2

Relation between the Moment of Inertia (J) and d

J (kgm^2)	d
0.007788	30
0.008012	40
0.0083	50
0.008613	60
0.008951	70
0.009314	80

Dynamics of the System

To continue with the analytics of the system, we need to determine a differential equation to describe the dynamics of the system.

The system which is the fuselage holding the battery with some of the other components needs to stabilize in pitch during hover mode. For this to happen, the wing that is connected to the servo motor will be making minor corrections to enable this stabilization.

In the figure above, the CG of the system is at a distance l from the tilt-wing axis. φ is the angle between the wing and the fuselage. h is the perpendicular distance between the wing and the CG.

The moment created by the motor on the wing will be equal to;

$$M = F \cdot h \quad (3.2)$$

From trigonometry

$$h = r \sin \varphi \quad (3.3)$$

If we assume that φ is a really small angle then

$$\sin \varphi = \varphi \quad (3.4)$$

Therefore,

$$M = Fr\varphi \quad (3.5)$$

Newton's 2nd law for rotational motion says that the sum of the torques on a rotating system about a fixed axis equals the product of the moment of inertia and the angular acceleration.

$$J\ddot{\theta} = M \quad (3.6)$$

Where J is the moments of inertia.

$\ddot{\theta}$ is the angular acceleration.

M is the torque or momentum.

To find a relation between the φ and newton's 2nd law for rotational motion, we equate equation to equation;

$$J\ddot{\theta} = Fr\varphi \quad (3.7)$$

$$\varphi = \frac{J\ddot{\theta}}{Fr} \quad (3.8)$$

The general equation for a PID controller is

$$u(t) = k_p e(t) + k_i \int_0^t e(\tau) d\tau + k_d \frac{d}{dt} e(t) \quad (3.9)$$

Where in our case we rewrite it to be;

$$\varphi(t) = k_p \theta(t) + k_i \int_0^t \theta(\tau) d\tau + k \frac{d}{dt} \theta(t) \quad (3.10)$$

θ which is the pitch angle is the controlled parameter, while φ which is the tilt-wing angle is the controlling parameter.

It should be noted that when $\varphi = 0$, the wing is vertical and there is no torque.

P- Controller with no Latency

The equation for a P controller with no latency will be;

$$\varphi = -[k_p\theta(t)] \quad (3.11)$$

$$\varphi(t) = -[k_p\theta(t)] \quad (3.12)$$

Since;

$$\varphi = \frac{J\ddot{\theta}}{Fr} \quad (3.13)$$

It can be rewritten as,

$$\frac{J\ddot{\theta}}{Fr} = -[k_p\theta(t)] \quad (3.14)$$

$$\ddot{\theta} = -\frac{Frk_p}{J}\theta(t) \quad (3.15)$$

If we write,

$$\frac{Frk_p}{J} = K_p \quad (3.16)$$

Then,

$$\ddot{\theta} + K_p\theta(t) = 0 \quad (3.17)$$

This becomes a 2nd order differential equation describing the dynamics of the system.

Solving the differential equation becomes the next step in finding out how the system reacts to just a P controller when there is no latency. This can be considered as an ideal case.

If we approximate,

$$\theta = e^{-mt} \quad (3.18)$$

Then,

$$\dot{\theta} = -me^{-mt} \quad (3.19)$$

$$\ddot{\theta} = m^2e^{-mt} \quad (3.20)$$

Equation becomes,

$$m^2e^{-mt} + K_p e^{-mt} = 0 \quad (3.21)$$

$$m^2 + K_p = 0 \quad (3.22)$$

Solving for m ,

$$m = \pm iK_p \quad (3.23)$$

The general solution for a differential equation with complex roots is,

$$\theta(t) = e^{\alpha t} [C_1 \cos(\beta)t + (iC_2 \sin(\beta)t)] \quad (3.24)$$

Therefore the solution for our system becomes,

$$\theta(t) = [C_1 \cos(K_p)^{\frac{1}{2}} t + (iC_2 \sin(K_p)^{\frac{1}{2}} t)] \quad (3.25)$$

P- Controller with Latency

There are a number of factors that could make the analytical data not match experimental data. These include; friction in the system, latency, imperfect performance of the servo motors, errors, and approximation and assumptions such as considering the wing with motors being weightless and having some moments of inertia.

In this thesis, latency is one of these factors that is considered in the analytics to try to get as close as possible to the actual data from the experiment.

A P- Controller is considered and a solution for the system is derived. The general equation for a P- Controller with latency is as shown below;

$$\ddot{\theta} + K_p\theta(t - \tau) = 0 \quad (3.26)$$

Solving this differential equation where;

$$\theta = e^{-mt} \quad (3.27)$$

$$m^2e^{-mt} + K_p e^{-mt} \cdot e^{-m\tau} = 0 \quad (3.28)$$

The characteristic equation becomes,

$$m^2 + K_p \cdot e^{-m\tau} = 0 \quad (3.29)$$

Using the approximation,

$$e^{-m\tau} \approx 1 - m\tau + \frac{m^2\tau^2}{2} \quad (3.30)$$

We get,

$$m^2 + K_p \left[1 - m\tau + \frac{m^2\tau^2}{2} \right] \quad (3.31)$$

$$m^2 + K_p - K_p m \tau + \frac{K_p m^2 \tau^2}{2} = 0 \quad (3.32)$$

$$m^2 + \frac{K_p m^2 \tau^2}{2} - K_p m \tau + K_p = 0 \quad (3.33)$$

Solving our equation in the form;

$$Ax^2 + Bx + c = 0 \quad (3.34)$$

$$\left(1 + \frac{K_p \tau^2}{2}\right) m^2 - K_p m \tau + K_p = 0 \quad (3.35)$$

Using the quadratic formula,

$$m_{1,2} = \frac{K_p \tau \pm \sqrt{K_p^2 \tau^2 - 4 \left[1 + \frac{K_p \tau^2}{2}\right] [K_p]}}{2 \left[1 + \frac{K_p \tau^2}{2}\right]} \quad (3.36)$$

The discriminant of the quadratic equation is determined to be less than zero. This indicates that the roots of the equation will be complex and the solution therefore is,

$$\theta(t) = e^{\frac{K_p \tau}{2 + K_p \tau^2}} \left[C_1 \cos\left(\frac{\sqrt{-4K_p - K_p^2 \tau^2}}{2 + K_p \tau^2}\right)(t) + i C_2 \sin\left(\frac{\sqrt{-4K_p - K_p^2 \tau^2}}{2 + K_p \tau^2}\right)(t) \right] \quad (3.37)$$

PD- Controller

A P controller, which is a proportional controller, only deals with the present error, a PD controller is more powerful since it gives a faster response and enables the system to stabilize easier than just a P controller.

The general equation for a PD controller is;

$$\varphi = -[k_p\theta(t) + k_d\dot{\theta}(t)] \quad (3.38)$$

$$\varphi(t) = -[k_p\theta(t) + k_d\dot{\theta}(t)] \quad (3.39)$$

Since;

$$\varphi = \frac{J\ddot{\theta}}{Fr} \quad (3.40)$$

It can be rewritten as,

$$\frac{J\ddot{\theta}}{Fr} = -[k_p\theta(t) + k_d\dot{\theta}(t)] \quad (3.41)$$

$$\ddot{\theta}(t) = -\frac{Frk_p}{J}\theta(t) - \frac{Frk_d}{J}\dot{\theta}(t) \quad (3.42)$$

Since;

$$\frac{Frk_p}{J} = K_p \quad (3.43)$$

$$\frac{Frk_d}{J} = K_d \quad (3.44)$$

Then the 2nd order differential equation describing the resulting dynamics of the system is;

$$\ddot{\theta}(t) + K_d\dot{\theta}(t) + K_p\theta(t) = 0 \quad (3.45)$$

Depending on physical parameters and coefficients k_p and k_d , there will be a sinusoidal that is either fading or increasing. From the 2nd-order differential equation, we can find an optimal relation between K_p and K_d .

The 2nd-order differential equation can be solved in the form,

$$\theta = e^{mt} \quad (3.46)$$

It becomes;

$$m^2 e^{mt} + K_d m e^{mt} + K_p e^{mt} = 0 \quad (3.47)$$

The characteristic equation is;

$$m^2 + K_d m + K_p = 0 \quad (3.48)$$

Solving the discriminant to get a relation between K_p and K_d , we get;

$$M_{1,2} = \frac{-K_d \pm \sqrt{K_d^2 - 4K_p}}{2} \quad (3.49)$$

$$K_d^2 - 4K_p = 0 \quad (3.50)$$

$$4K_p = K_d^2 \quad (3.51)$$

$$K_p = \frac{K_d^2}{4} \quad (3.52)$$

CHAPTER IV

Methodology

The test bench was initially designed in SOLIDWORKS for several reasons: the parts going into the fuselage should be carefully placed and the electrical components should be fixed. Movement of these components would disrupt the moments of the aircraft leading to errors in the experiment. The figures below show the right, front, and top view of the fuselage with the battery holder.

Figure 4.1

A Right-Side View of the Fuselage with the Battery Holder

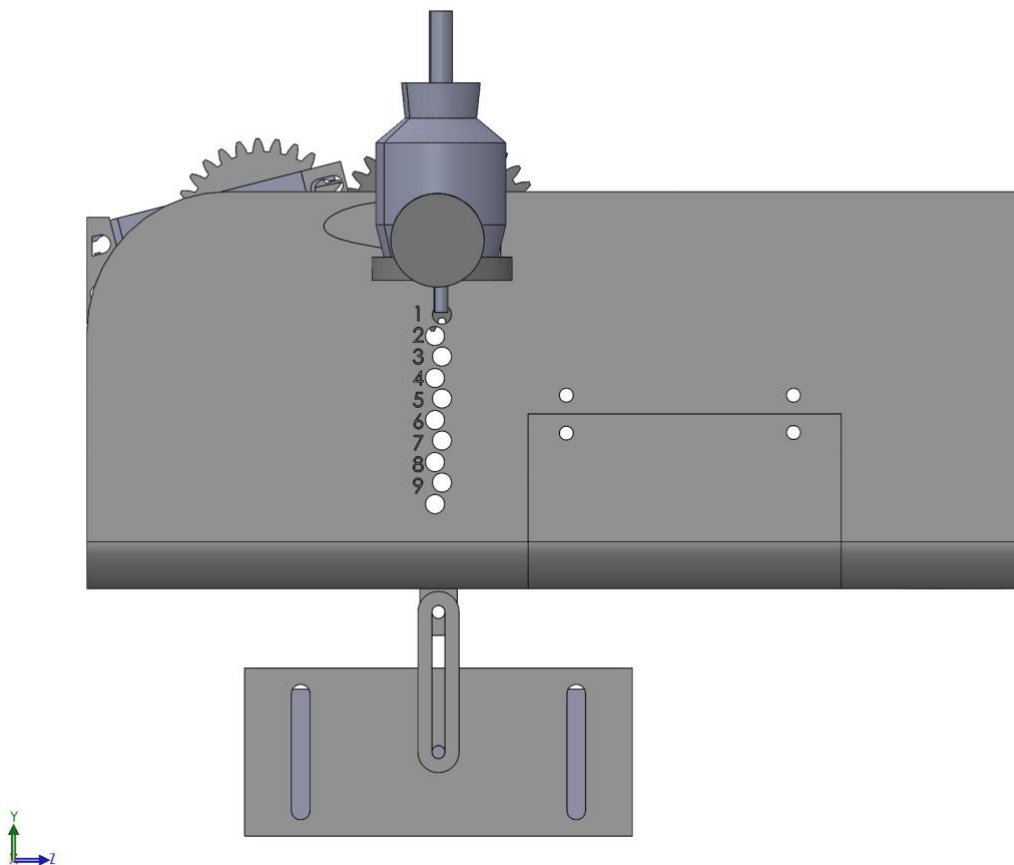


Figure 4.2

A front View of the Fuselage with the Battery Holder.

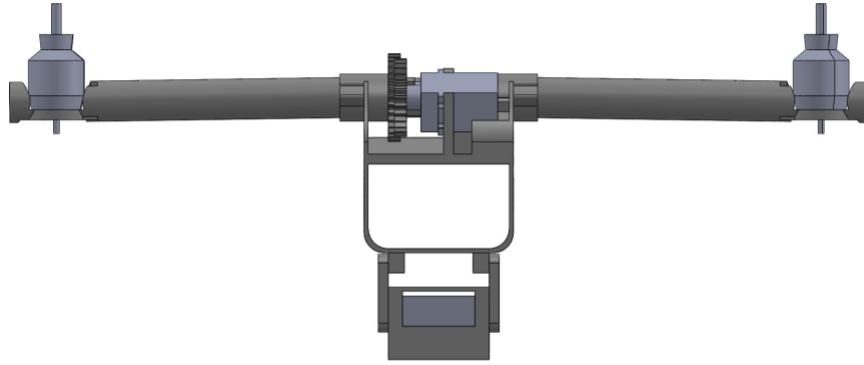
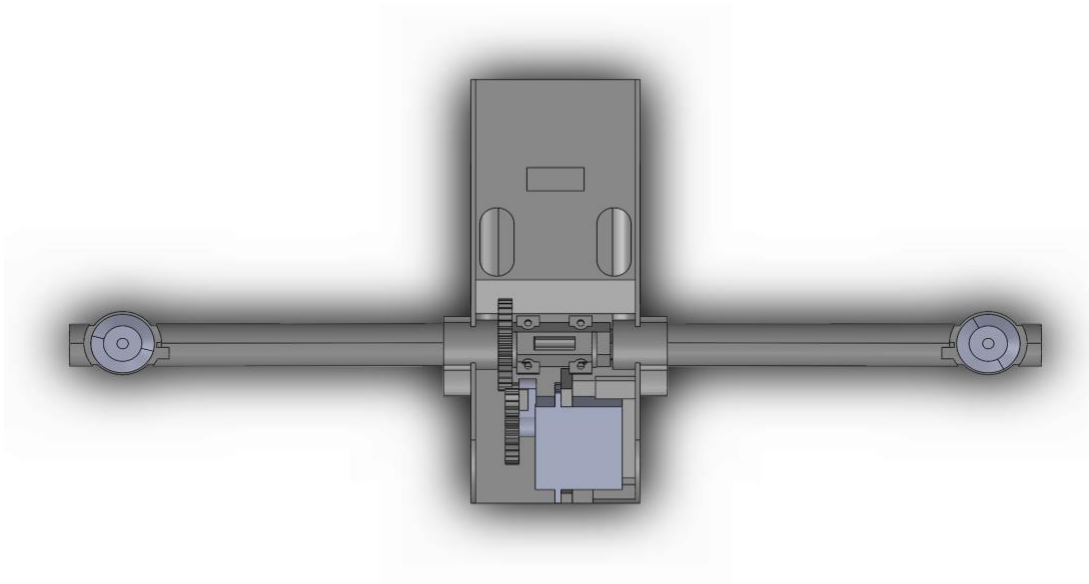


Figure 4.3

A Top View of the Fuselage.



Components used in the UAV

Several electrical components are used in the UAV. They are

i) Servo Motor

A servo motor is a closed-loop servo mechanism that uses position feedback to control its motion and final position (“Servo motor”, n.d). In the tilt-wing UAV, the servo motor is attached to a gear. This gear turns another gear attached to the wing to facilitate the tilt-wing motion of the aircraft. The gears are in the ratio of 1.8:1.

Figure 4.4

Servo Motor



ii) ESC

An electronic speed controller (ESC) controls and regulates the speed of the motors (Andrew Gong and Dries Verstraete, 2017).

Figure 4.5

Example of an ESC

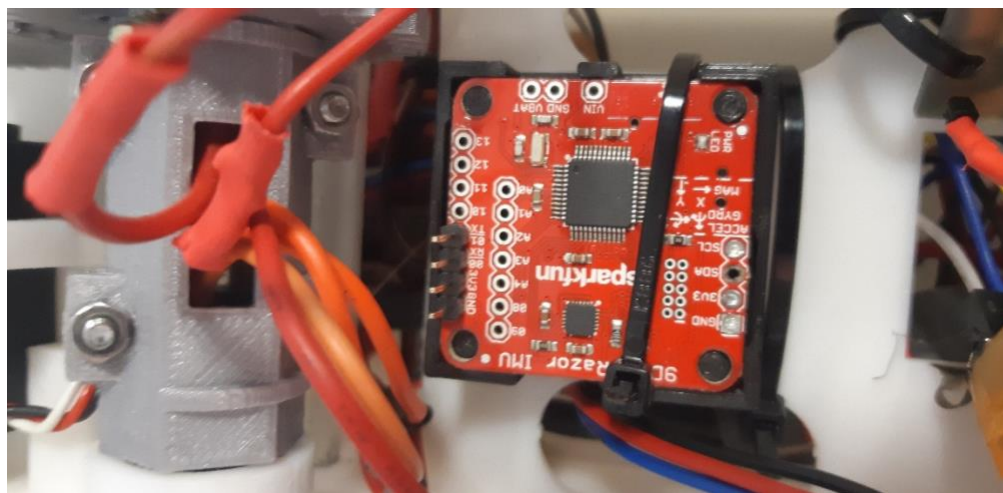


iii) IMU

An inertial measurement unit (IMU) is a device that contains an accelerometer, gyroscope, and magnetometer. It measures specific gravity and the angular rate of the object that it is attached to. This device on the UAV helps in determining the position of the UAV. It sends its data to the flight controller and necessary corrections are then made to the tilt-wing to bring the aircraft to stable flight in hover mode (N. Ahmad et al., 2013).

Figure 4.6

An Inertial Measurement Unit (IMU)



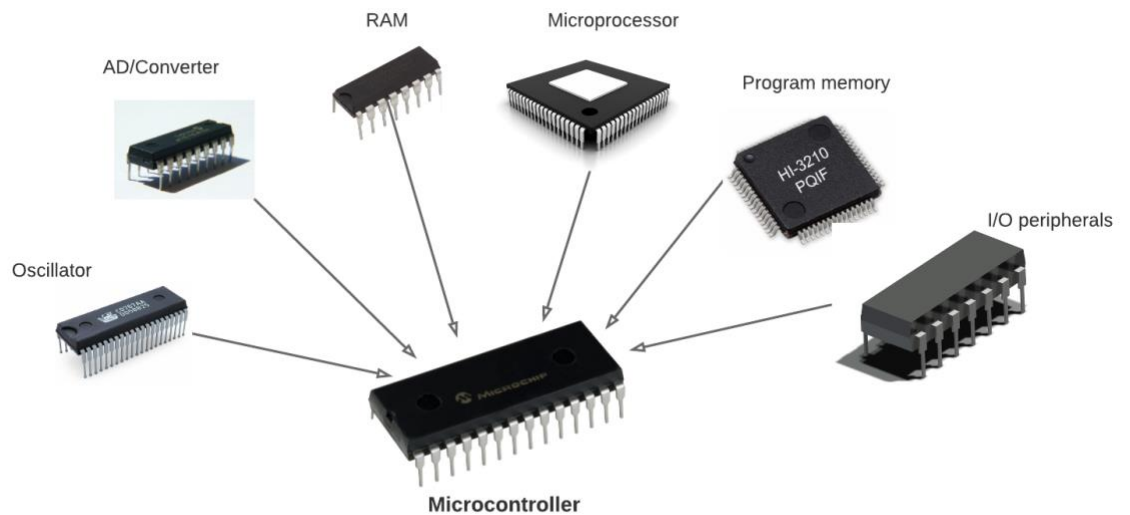
If the UAV is pitching down, the IMU will show a negative pitch angle, and the wing will tilt backward to make the aircraft react and come to a stable flight. If the UAV is pitching up, the IMU will show a positive pitch angle, and the wing will tilt forward to bring back the aircraft into stable flight.

iv) Microcontroller

A microcontroller is a compressed microcomputer that is used to control the functions of a system. In our case, the microcontroller used is a teensy board. Teensy is a USB-based microcontroller capable of implementing many types of projects (“Microcontroller”, n.d). The microcontroller is comprised of a number of

components. These include an oscillator, AD/ converter, RAM, Microprocessor, program memory and Input output peripherals.

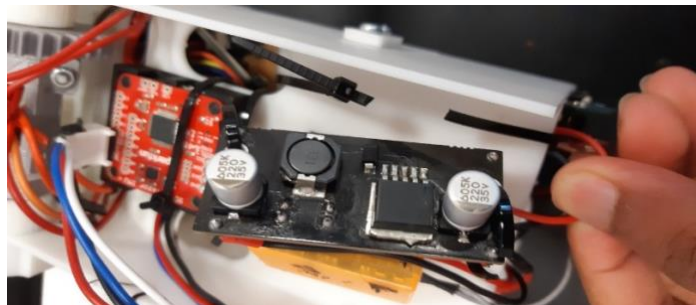
Figure 4.7
Microcontroller (“Circuit basics”, n.d)



v) Voltage Regulator

A voltage regulator is a system designed to automatically maintain a constant voltage (“voltage regulator”, n.d). In the UAV 2 voltage regulators were used. One of 3 volts and the other of 5 volts.

Figure 4.8
3V Voltage Regulator



vi) Receiver

Drone receivers are electronic components that receive signals from the drone's remote control and translate them into commands for the drone's flight controller. The flight controller then adjusts the UAV's motors and other systems like the tilt-wing and thrust differential to respond to the pilot's commands. Receivers typically use radio frequency signals to communicate with the remote control, and they come in different types and frequencies to suit different drone designs and use cases. Some advanced drone receivers may also incorporate features like telemetry feedback or multiple input channels for more precise control.

Figure 4.9

Radio Receivers. ("robocraze", n.d)



vii) Remote Controller

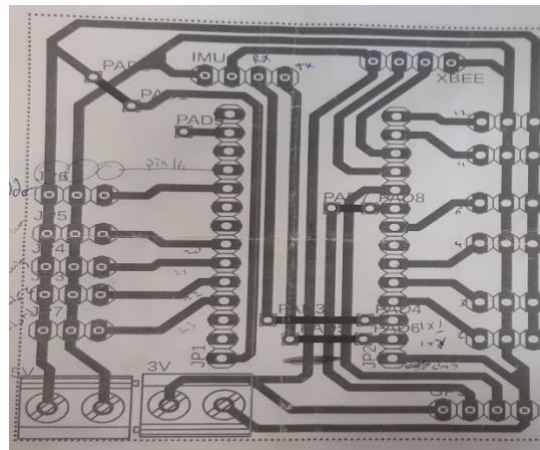
The Remote controller is used to send signals to the drone's receiver, which in turn interprets the pilot's inputs and relays them to the drone's flight controller. Which is the brain of the system. It typically includes buttons and a joystick that the pilot can use to control the UAV. It allows the pilot to change the drone's speed, altitude, direction, and tilt-wing angle among others. It communicates with the drone's receiver using radio frequency signals.

Figure 4.10
Remote Controller



The figure shown below shows the PCB design layout used in the project.

Figure 4.11
PCB Layout



The first step in the experiment is to put the test bench in neutral equilibrium. Stability can be categorized into; static stability and dynamic stability (J B Russell 1996). Static stability can be further divided into positive static stability, negative static stability, and neutral static stability. Positive static stability is the tendency of an object to return back to its initial position after a disturbance. Negative static stability is the tendency of an object to not return back to its initial position but continue moving away from the original point.

Neutral equilibrium is a type of equilibrium that happens when a body that is subjected to an external force comes to rest at that new position. Examples of neutral equilibrium include a ball lying on the ground. An external force is required for the ball to move. Hence this is a neutral equilibrium. Another example is a marble lying on a horizontal surface, undisturbed. An external force is also required to move the marble.

The fuselage and battery holder together with the stands for which the fuselage is mounted to are 3d printed using PLA. It is a readily available material that is used in 3d printing. Its best characteristics are that it is easy to print with, it can be printed at relatively low temperatures, and it is also mechanically strong. These are some of the reasons why PLA was one of the best materials to use in 3d printing.

Design of the Test bench

The fuselage together with the battery holder is held by the test bench stand. Several iterations of the stand were designed in SOLIDWORKS to come up with the best model. The ideal characteristics of the stand would be one that is tall enough to allow the easy movement of the system. It would also have to be rigid enough to prevent vibrations in the system. It needs to be firmly fixed to the base.

The stand is required to also be heavier than the amount of force that the motors can produce. This is to prevent it from lifting in the air. Something that might end up being catastrophic. The stand and the fuselage are connected by a 3.5mm aluminum rod that passes through both of them. This facilitates the easy rotation of the fuselage.

To prevent the fuselage from toppling over when the motors and propellers are spinning, stoppers are designed and fixed to the stands. These allow the fuselage to have a pitch angle of $\pm 30^\circ$.

The figures below show the right, and front views of the test bench stand.

Figure 4.12

Right and Front Views of the Test Bench Stand.

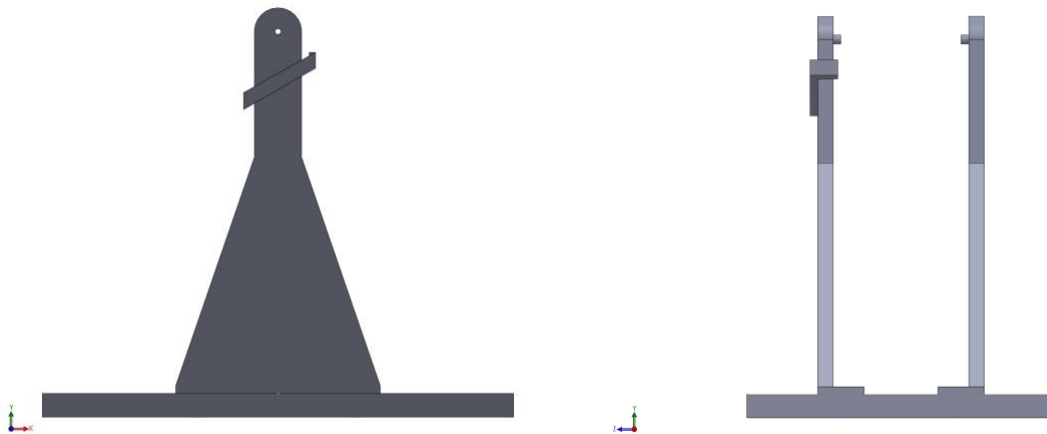
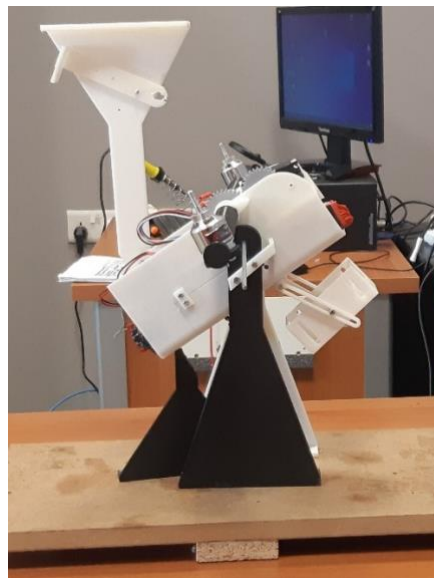


Figure 4.13

Fuselage Mounted on the Test Bench Stand.



Delay Estimation

One of the errors that are present in the experiment is latency. This can be defined as the time taken for a system to respond to a command. (Luca Bigazzi et al, 2021) elaborated that the latency in their system negatively affected the position controller that exploits data from the computer vision system, preventing its usage for precise positioning applications.

In order to determine the latency in this system, just a P-Controller is used. This is because it would make it easier in finding out the latency. A number of tests at different P coefficients are done.

In this experiment, an initial P coefficient of 0.5 was used and the system's response was observed. Its period and amplitude data were derived from the IMU and the graph of amplitude against period is derived. This experiment is repeated for P coefficients 0.4 and 0.3.

CHAPTER V

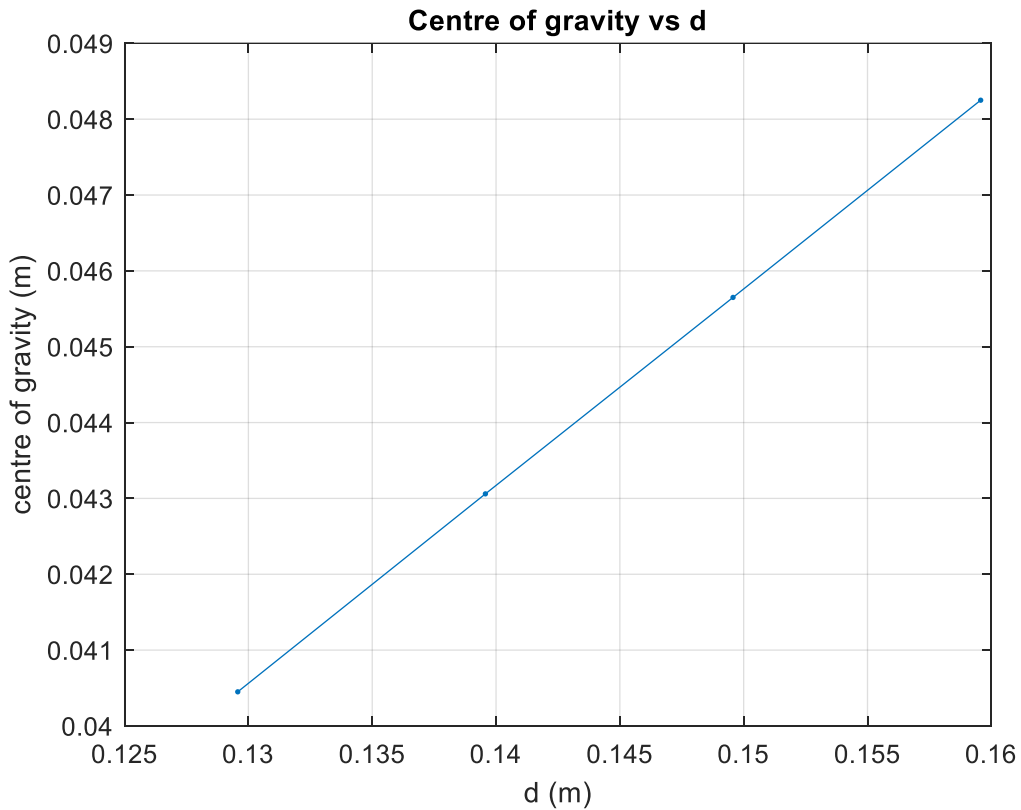
Results and Discussion

One of the first things looked at is the relation between 'd' and 'l'. The position of the battery to the tilt-wing axis and the distance between the CG of the system and the tilt-wing axis. A linear relation is observed between these two parameters. As the battery is moved lower, the CG of the system will also move down. The reverse is also seen to be true.

The graph below shows the relation between these two parameters.

Figure 5.1

Centre of Gravity (l) against d.

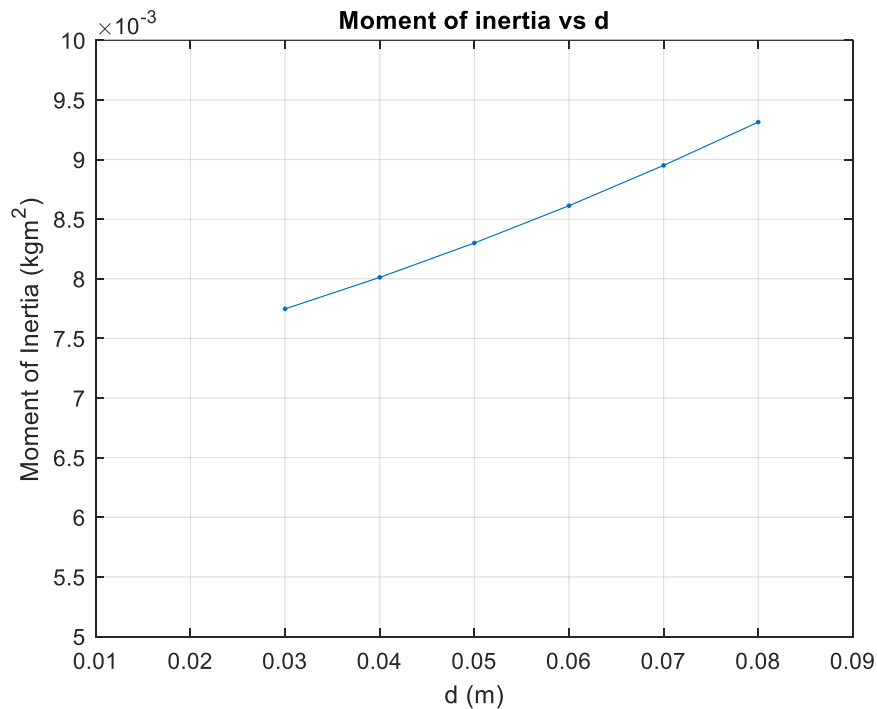


The relation between the moment of inertia and distance 'd' was also investigated. The moment of inertia of the system taken at the CG is found to be linearly related to the distance between the tilt-wing axis and the position of the battery (d). This is however not in match with the theory. In the formula for the moment of inertia, it can be seen that this relation should be quadratic. The

reason why it might be seen as linear could be because the battery is not heavy enough compared to the rest of the fuselage to influence the results and hence the part shown in the graph is only part of the parabola. The graph below shows this relation.

Figure 5.2

Moment of Inertia (J) against d.



The graphs below in figure 5.3, 5.4, 5.5 show the comparison between the theoretical and the experimental response of the P controller in the pitch control of the experiment. From the theoretical work done, it can be observed that a system with just a P controller and possessing latency will have a sinusoidal oscillations that are increasing exponentially. This is what is observed in the experiment. It is only visible to a certain point because of the stoppers used in the experiment that prevent the fuselage from overturning.

The experimental values are within a margin of reason. The difference between the two can be easily attributed to a number of factors. These are; the presence of friction in the setup that was not considered in the theoretical work. Secondly, the imperfect performance of the servo motors. Thirdly, the moment of inertia from the wings was not considered in the initial analytics. This was found to be an error and hence should be considered in future work. The assumption that the

wing with motors is weightless and in turn its moment of inertia could be ignored was found to not be correct.

The P controller with a k_p value of 0.4 is found to respond slower to any disturbance than the ones with higher k_p values. This is an observation that is in line with the theoretical work.

Figure 5.3

Comparison between Experimental and Theoretical Data for k_p value 0.4

Comparison between experimental and theoretical data for 0.4 P coefficient

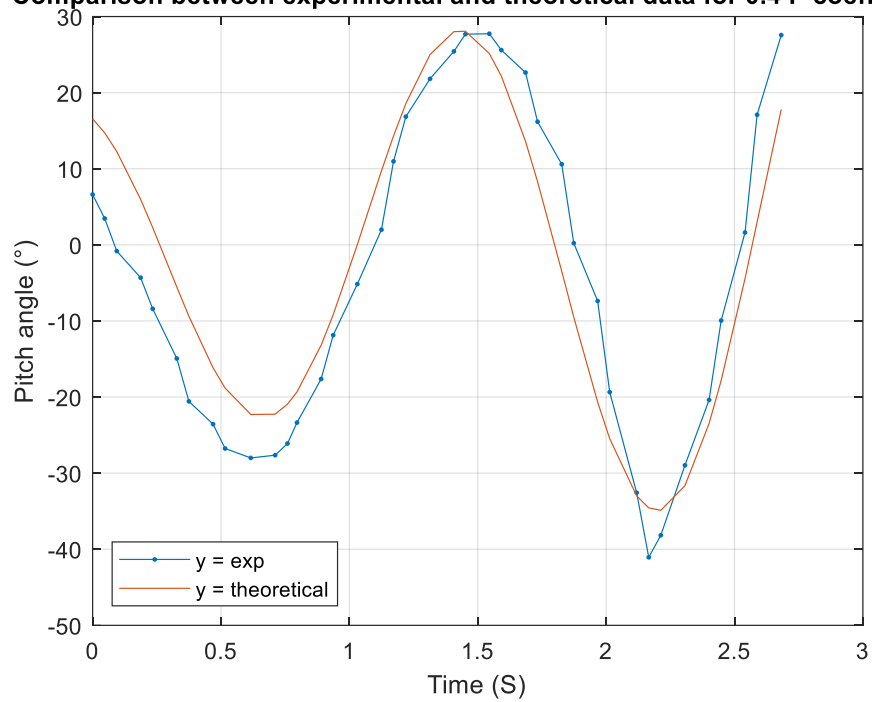


Figure 5.4

Comparison between Experimental and Theoretical Data for k_p value 0.5

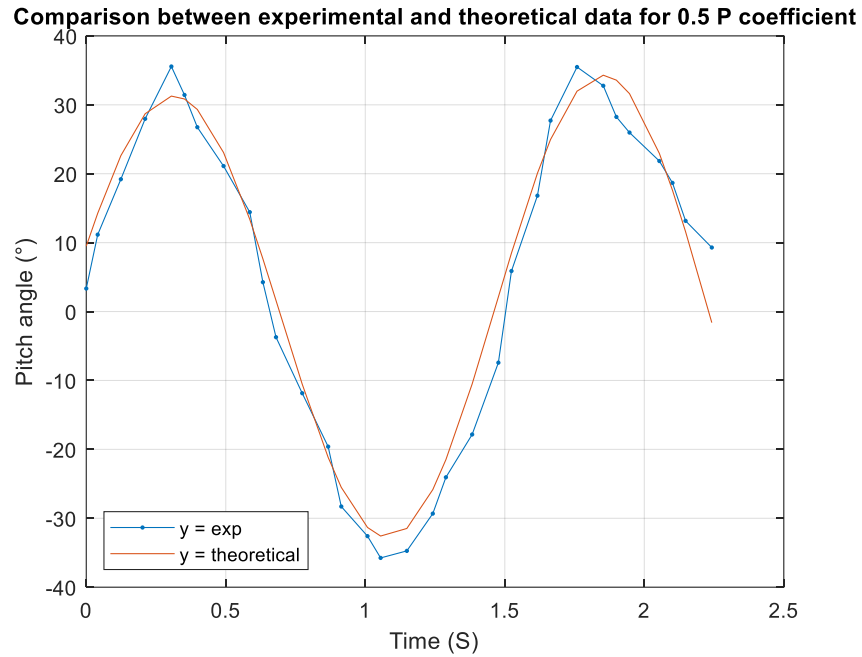


Figure 5.5

Comparison between Experimental and Theoretical Data for k_p value 0.6

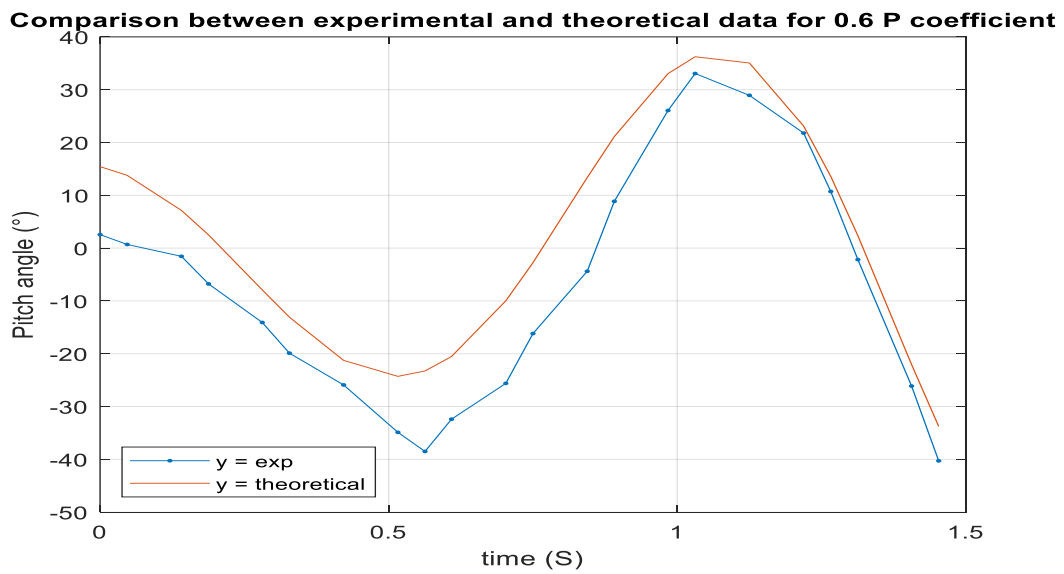


Table 5.1

Comparison of the k_p Values

	0.4	0.5	0.6
Standard deviation experimental	20.64567	23.08258	22.34313
Standard deviation theoretical	19.29958	22.2042	21.12483

CHAPTER VI

Conclusion

The Near East University Laboratory is developing a tilt-wing VTOL UAV named LANNER for various purposes such as surveillance, border patrol, and farming. To test for pitch control in this hybrid UAV, a test-bench was designed using SOLIDWORKS. Previous tests on LANNER showed that a test-bench dedicated to pitch control was needed as the UAV had good control in roll but not as good in pitch control.

In this thesis, a test-bench was designed by the use of SOLIDWORKS to test for pitch control in a tilt wing UAV. The hybrid UAV is capable of vertically taking off and landing.

In this study pitch control in hover flight is the main subject of interest. A comparison between the theoretical work and the experimental work done showed good results between the two. P Controller with k_p values of 0.4, 0.5 and 0.6 was implemented and the results were looked at to check for the validity of the experiment and if it compared well to the theoretical work.

The effect of the distance between the battery and the CG of the system during transition mode is also briefly looked at. In transition mode, when the wing has just fully transitioned into airplane mode and the distance between the CG is great, a larger force is required by the horizontal stabilizer to stabilize the plane compared to when the battery is closer to the CG of the system.

Future work into this project should include an addition of the moments of inertia of the wings into the analytical work to get a better comprehension of the system. The PID controller should be implemented and a test done outside to see how the UAV responds.

References

- A. L. Salih, M. Moghavvemi, H. A. F. Mohamed and K. S. Gaeid, "Modelling and PID controller design for a quadrotor unmanned air vehicle," 2010 IEEE International Conference on Automation, Quality and Testing, Robotics (AQTR), 2010, pp. 1-5, doi: 10.1109/AQTR.2010.5520914.
- Borase, Rakesh & Maghade, Dilip & Sondkar, Shilpa & Pawar, Sushant. (2021). A review of PID control, tuning methods and applications. *International Journal of Dynamics and Control*. 9. 10.1007/s40435-020-00665-4.
- Cornelius A. Thiels, Johnathon M. Aho, Scott P. Zietlow, Donald H. Jenkins, Use of Unmanned Aerial Vehicles for Medical Product Transport, *Air Medical Journal*, Volume 34, Issue 2, 2015, Pages 104-108, ISSN 1067-991X, <https://doi.org/10.1016/j.amj.2014.10.011>. (<https://www.sciencedirect.com/science/article/pii/S1067991X14003332>)
- D. Dantsker, Moiz Vahora, Saym Imtiaz and Marco Caccamo. "[High Fidelity Moment of Inertia Testing of Unmanned Aircraft](#)," AIAA 2018-4219. *2018 Applied Aerodynamics Conference*. June 2018.
- [De Wagter, C. Paredes-Valles, F. Sheth, N. et al \(2021\)](#) Learning fast in autonomous drone racing. <https://doi.org/10.1038/s42256-021-00405-z>
- E. Cetinsoy, S. Dikyar, C. Hancer, K.T. Oner, E. Sirimoglu, M. Unel , M.F. Aksit (2012) Design and construction of a novel quad tilt-wing UAV <https://doi.org/10.1016/j.mechatronics.2012.03.003>.
- E. Small, E. Fresk, G. Andrikopoulos and G. Nikolakopoulos, "Modelling and control of a Tilt-Wing Unmanned Aerial Vehicle," 2016 24th Mediterranean Conference on Control and Automation (MED), 2016, pp. 1254-1259, doi: 10.1109/MED.2016.7536050.
- Erceg, Aleksandar & Činčurak Erceg, Biljana & Vasilj, Aleksandra. (2017). Unmanned Aircraft Systems in Logistics – Legal Regulation and Worldwide Examples Toward Use in Croatia.

- Gabl, R., Davey, T., Nixon, E., & Ingram, D. M. (2021). Accuracy Analysis of the Measurement of Centre of Gravity and Moment of Inertia with a Swing. *Applied Sciences*, 11(12), 5345. MDPI AG. Retrieved from <http://dx.doi.org/10.3390/app11125345>
- Hegde, N.T., George, V.I., Nayak, C.G. and Kumar, K. (2020), "Design, dynamic modelling and control of tilt-rotor UAVs: a review", *International Journal of Intelligent Unmanned Systems*, Vol. 8 No. 3, pp. 143-161. <https://doi.org/10.1108/IJIUS-01-2019-0001>
- Kontogiannis, Spyridon & Ekaterinaris, John. (2013). Design, performance evaluation and optimization of a UAV. *Aerospace Science and Technology*. 29. 339-350. 10.1016/j.ast.2013.04.005.
- M. A. Ma'sum *et al.*, "Simulation of intelligent Unmanned Aerial Vehicle (UAV) For military surveillance," *2013 International Conference on Advanced Computer Science and Information Systems (ICACSIS)*, 2013, pp. 161-166, doi: 10.1109/ICACSIS.2013.6761569.
- Microcontroller, Circuit basics. (2023, February 13). <https://www.circuitbasics.com/introduction-to-microcontrolleres/>
- Microcontroller. (2022, December 25). In *Wikipedia*. <https://en.wikipedia.org/wiki/Microcontroller>
- Mohsan, S. A. H., Khan, M. A., Noor, F., Ullah, I., & Alsharif, M. H. (2022). Towards the Unmanned Aerial Vehicles (UAVs): A Comprehensive Review. *Drones*, 6(6), 147. MDPI AG. Retrieved from <http://dx.doi.org/10.3390/drones6060147>
- Norhafizan Ahmad, Raja A. R. Ghazilla, Nazirah M. Khairi. Review on various Inertial Measurement Unit (IMU) Sensor Applications. *International Journal of Signal Processing Systems* Vol.1, No 2. December 2013.
- Servo Motor. (2023, February 13). In *Wikipedia*. <https://en.wikipedia.org/wiki/Servomotor>
- S. Y. Choi & D. Cha (2019) Unmanned aerial vehicles using machine learning for autonomous flight; state-of-the-art <https://doi.org/10.1080/01691864.2019.1586760>

Sanchez-Rivera, L. M., Lozano, R., & Arias-Montano, A. (2020). Development, Modeling and Control of a Dual Tilt-Wing UAV in Vertical Flight. *Drones*, 4(4), 71. MDPI AG. Retrieved from <http://dx.doi.org/10.3390/drones4040071>

Tae H. Ha, Keunseok Lee and John T. Hwang (2019). Large-scale design economics optimization of evtol concepts for urban air mobility. <https://doi.org/10.2514/6.2019-1218>. University of California San Diego, La Jolla, CA, 92122

Transition Flight Of Quad Tilt Wing Vtol UAV Koji Muraoka*, Noriaki Okada*, Daisuke Kubo* and Masayuki Sato* *Japan Aerospace Exploration Agency
muraoka.koji@jaxa.jp

Tsouros, D. C., Bibi, S., & Sarigiannidis, P. G. (2019). A Review on UAV-Based Applications for Precision Agriculture. *Information*, 10(11), 349. MDPI AG. Retrieved from <http://dx.doi.org/10.3390/info10110349>

U. Ozdemir et al., "Design of a commercial hybrid VTOL UAV system," 2013 International Conference on Unmanned Aircraft Systems (ICUAS), 2013, pp. 214-220, doi:10.1109/ICUAS.2013.6564693.

William J. Fredericks David D. North, Mark A. Agate, Zachary R. Johns NASA Langley Research Center, Hampton, VA, 23681 Transformational Flight ATIO AIAA Aviation 2015 Conference13 Advanced Concepts Session

Appendices

Appendix A. MATLAB Code for the Comparison between Theory and Experimental Data For 0.5 P Coefficient.

```

close all
clear

dat = importdata('pitch5trial2.txt');

tvec = dat(:,2)/1000;
angvec = dat(:,1);

%manually put time limits
tmin = 22.5;
tmax = 26.5;

%cut out the zone of interest
zone_inds = (tvec >= tmin) & (tvec <= tmax);
tvec = tvec(zone_inds);
angvec = angvec(zone_inds);

tvec = tvec - tvec(1); %now time will start from 0

figure
plot(tvec, angvec, '.-'); grid on

Fcost_opt = +Inf;

for A = 25:0.1:35

    %DEBUG:
    A

    for freq = 0.8:0.05:1.2
        for phi = 2*pi*(0:0.05:1)
            for alpha = -0.5:0.02:0.5

                theta_theor = A * (cos((2*pi*freq .* tvec) + phi)) .*
(exp(alpha * tvec));
                Fcost = sum((angvec - theta_theor).^2);

                if Fcost < Fcost_opt
                    Fcost_opt = Fcost;
                    A_opt = A;
                    freq_opt = freq;
                    phi_opt = phi;
                    alpha_opt = alpha;
                end
            end
        end
    end
end
end
end
end

```

```
theta_opt = A_opt * (cos((2*pi*freq_opt .* tvec) + phi_opt)) .*  
(exp(alpha_opt * tvec));  
  
figure  
plot(tvec, angvec, '.-'); grid on; hold on  
plot(tvec, theta_opt, '-')
```

Appendix B. MATLAB Code for the Comparison between Theory and Experimental Data For 0.6 P Coefficient.

```

close all
clear

dat = importdata('pitch6trial3.txt');

tvec = dat(:,1)/1000;
angvec = dat(:,5);

% plot(tvec, angvec, '-'); grid on

%manually put time limits
tmin = 11.6;
tmax = 13.7;

%cut out the zone of interest
zone_inds = (tvec >= tmin) & (tvec <= tmax);
tvec = tvec(zone_inds);
angvec = angvec(zone_inds);

tvec = tvec - tvec(1); %now time will start from 0

figure
plot(tvec, angvec, '-'); grid on

Fcost_opt = +Inf;

for A = 35:0.1:45

    %DEBUG:
    A

    for freq = 0.8:0.05:1.2
        for phi = 2*pi*(0:0.001:1)
            for alpha = -0.5:0.02:0.5

                theta_theor = A * (cos((2*pi*freq .* tvec) + phi)) .*
(exp(alpha * tvec));
                Fcost = sum((angvec - theta_theor).^2);

                if Fcost < Fcost_opt
                    Fcost_opt = Fcost;
                    A_opt = A;
                    freq_opt = freq;
                    phi_opt = phi;
                    alpha_opt = alpha;
                end
            end
        end
    end
end
end
end
end

```

```
theta_opt = A_opt * (cos((2*pi*freq_opt .* tvec) + phi_opt)) .*  
(exp(alpha_opt * tvec));  
  
figure  
plot(tvec, angvec, '.-'); grid on; hold on  
plot(tvec, theta_opt, '-')
```


Appendix C. MATLAB Code for the Comparison between Theory and Experimental Data For 0.4 P Coefficient.

```

dat = importdata('pitch4trial1.txt');

tvec = dat(:,1)/1000;
angvec = dat(:,2);

%manually put time limits
tmin =30;
tmax = 31.8;

%cut out the zone of interest
zone_inds = (tvec >= tmin) & (tvec <= tmax);
tvec = tvec(zone_inds);
angvec = angvec(zone_inds);

tvec = tvec - tvec(1); %now time will start from 0

figure
plot(tvec, angvec, '.-'); grid on

Fcost_opt = +Inf;

for A = 20:0.1:28

    %DEBUG:
    A

    for freq = 0.5:0.05:1.0
        for phi = 2*pi*(0:0.01:1)
            for alpha = -0.5:0.02:0.5

                theta_theor = A * (cos((2*pi*freq .* tvec) + phi)) .*
(exp(alpha * tvec));
                Fcost = sum((angvec - theta_theor).^2);

                if Fcost < Fcost_opt
                    Fcost_opt = Fcost;
                    A_opt = A;
                    freq_opt = freq;
                    phi_opt = phi;
                    alpha_opt = alpha;
                end
            end
        end
    end

end

theta_opt = A_opt * (cos((2*pi*freq_opt .* tvec) + phi_opt)) .*
(exp(alpha_opt * tvec));

figure

```

```
plot(tvec, angvec, '.-'); grid on; hold on  
plot(tvec, theta_opt, '-')
```

Appendix D. Code for the PID

```
#ifndef VTOL_HOVER_H
#define VTOL_HOVER_H

//ATTENTION: X - front, Y - up, Z - right

float J = 0.0076; //inertia moment along Z-axis

float F0 = 5;

float L = 0.022;

float Lmotor = 0.18; //distance from CG to motor

float Jroll = 0.02; //inertia moment along X-axis

float roll_coef_p = 0.00; //0.15;

float roll_Coef_P = roll_coef_p * F0*Lmotor/Jroll;

float roll_Coef_D = sqrt(3*roll_Coef_P);

float roll_Coef_I = roll_Coef_D*roll_Coef_D*roll_Coef_D / 27;

float roll_coef_d = roll_Coef_D * Jroll/(F0*Lmotor);

float roll_coef_i = roll_Coef_I * Jroll/(F0*Lmotor);

float roll_coef_p_scaled = roll_coef_p / 57.3;

float roll_coef_d_scaled = roll_coef_d * 50.0/57.3;

float roll_coef_i_scaled = roll_coef_i / (50.0 * 57.3);
```

```

//! coef_p = 0.25 and 0.8 in front of coef_d give good result(pitch)

//float pitch_coef_p = 0.25;

//float pitch_Coef_P = pitch_coef_p * F0*L/J;

//float pitch_Coef_D = 2*sqrt(pitch_Coef_P);

//float pitch_coef_d = 0.8 * pitch_Coef_D * J/(F0*L);

//float pitch_coef_i = 0.0;

float pitch_coef_p = 0.15; //0.25; //0.4 - for testbench, and 0.2 - presumably for flight;

float pitch_Coef_P = pitch_coef_p * F0*L/J;

float pitch_Coef_D = sqrt(3*pitch_Coef_P);

float pitch_Coef_I = pow(pitch_Coef_D,3)/27;

float pitch_coef_d = 0.5 * pitch_Coef_D * J/(F0*L);

float pitch_coef_i = pitch_Coef_I * J/(F0*L); //0.4

float pitch_coef_p_scaled = (pitch_coef_p / 57.3) / 1.2;

float pitch_coef_d_scaled = (pitch_coef_d * 50.0/57.3) / 1.2;

float pitch_coef_i_scaled = 0 * pitch_coef_i / (50.0 * 57.3) / 1.2;

pid_controller<float> pid_hoverpitch(pitch_coef_p_scaled, pitch_coef_i_scaled,
pitch_coef_d_scaled,

-90.0, 90.0, -0.99, 0.99, false, 0.0);

```

```
pid_controller<float> pid_hoverroll(roll_coef_p_scaled, roll_coef_i_scaled, roll_coef_d_scaled,  
                                   -90.0, 90.0, -0.99, 0.99, false, 0.0);
```

```
class vtol_hover {  
  
    void (vtol_hover::* state)();  
  
    void stby() {  
  
        servo_ch4(rc_ch2() + rc_ch3());  
  
        servo_ch4(rc_ch2() - rc_ch3());  
  
  
        //servo_ch4(rc_ch2());  
  
        //servo_ch5(rc_ch2());  
  
  
        //'equalized' motor steering  
  
        //auto handle_throttle = math::map<float>(rc_ch2(), -0.61, 0.84, 1, 0);  
  
        //auto diff_throttle = rc_ch3();  
  
        //auto throttle_left = math::map<float>(handle_throttle*(1 - diff_throttle), 1, 0, -0.4, 0.8);  
  
        //auto throttle_right = math::map<float>(handle_throttle*(1 + diff_throttle), 1, 0, -0.2, 0.45);  
  
  
        servo_ch3(rc_ch5());  
  
        servo_ch2(rc_ch4());  
  
    }  
};
```

```
//servo_ch2(rc_ch3());

telemetry_write_ping(imu.roll_raw, imu.pitch_raw, imu.yaw_raw, imu.corr,
                    control_enb(), rc_ch2(), 0, 0, 0, 0);

if (control_enb())
    state = &vtol_hover::boot;
}

void boot() {
    pid_hoverpitch.reset();
    pid_hoverroll.reset();
    state = &vtol_hover::step;
}

void step() {
    auto pitch_target = math::map_rev<float>(rc_ch5(), -1, 1, -50, 30);
    auto roll_target = math::map_rev<float>(rc_ch3(), -1, 1, -30, 30);

    //pitch PID
    pid_hoverpitch.set_setpoint(pitch_target);

    auto pitch_signal = pid_hoverpitch.step(imu.pitch_raw);
```

```
//roll PID

pid_hoverroll.set_setpoint(roll_target);

    auto roll_signal = pid_hoverroll.step(imu.roll_raw);

//scaling the throttle handle input for motors

auto handle_throttle = math::map_rev<float>(rc_ch2(), 0.84, -0.61, 0, 1);

auto throttle_left = math::map_rev<float>(handle_throttle*(1 + roll_signal), 1, 0, -0.19, 0.17);

auto throttle_right4left = math::map_rev<float>(handle_throttle*(1 - roll_signal), 1, 0, -0.19,
0.17);

auto throttle_right = 0.00;

if (throttle_left > 0.15) {

    throttle_right = math::map_rev<float>(throttle_right4left, 0.15, 0.10, 0.385, 0.27);

}

else if (throttle_left > 0.05) {

    throttle_right = math::map_rev<float>(throttle_right4left, 0.10, 0.05, 0.27, 0.20);

}

else if (throttle_left > 0.00) {

    throttle_right = math::map_rev<float>(throttle_right4left, 0.05, 0.00, 0.20, 0.08);

}

else if (throttle_left > -0.05) {

    throttle_right = math::map_rev<float>(throttle_right4left, 0.00, -0.05, 0.08, 0.00);

}

else if (throttle_left > -0.10) {
```

```
throttle_right = math::map_rev<float>(throttle_right4left, -0.05, -0.10, 0.00, -0.13);
}

else if (throttle_left > -0.15) {
throttle_right = math::map_rev<float>(throttle_right4left, -0.10, -0.15, -0.13, -0.20);
}

else {
throttle_right = math::map_rev<float>(throttle_right4left, -0.15, -0.19, -0.20, -0.30);
}

//throttle_left = -0.06;

//throttle_right = 0.08;

//auto throttle_right = math::map<float>(handle_throttle*(1 + roll_signal), 1, 0, -0.2, 0.45);

//auto throttle_left = math::map<float>(handle_throttle*(1 - roll_signal), 1, 0, -0.4, 0.8);

//pid_test.set_setpoint();

//auto roll_signal = pid_test.step(imu.roll_raw);

//servo_ch3(rc_ch5()); //UAV ailerons

servo_ch3(0.28 + pitch_signal); //tiltwing (we had 0.65 as neutral point)

//servo_ch3(-0.35);
```



```
servo_ch4(0.3); //channel for both motors when working on testbench 2

//servo_ch4(throttle_left); //left motor

//servo_ch5(throttle_right); //right motor

// TELEMETRY_STREAM.print((0.22 + roll_signal));

// TELEMETRY_STREAM.print(" ");

// TELEMETRY_STREAM.print((0.12 - roll_signal));

// TELEMETRY_STREAM.println("");

telemetry_write_ping(imu.roll_raw, imu.pitch_raw, imu.yaw_raw, imu.corr,
                    control_enb(), rc_ch2(), rc_ch3(), rc_ch4(), rc_ch5(), control_enb());

//telemetry_write_pid_state(pid_roll, pid_pitch);

if (!control_enb())
    state = &vtol_hover::stby;
}

void shutdown() { }
```

```
public:
```

```
    vtol_hover() : state(&vtol_hover::stby) {}
```

```
    void operator() {(this->*state)();}
```

```
}hover;
```

```
#endif
```

Appendix X. Turnitin Report



[Assignments](#)
[Students](#)
[Grade Book](#)
[Libraries](#)
[Calendar](#)
[Discussion](#)
[Preferences](#)

NOW VIEWING: HOME > PAPER > AHMED-ZAKWAN

About this page

This is your assignment inbox. To view a paper, select the paper's title. To view a Similarity Report, select the paper's Similarity Report icon in the similarity column. A ghosted icon indicates that the Similarity Report has not yet been generated.

AHMED-ZAKWAN

INBOX | NOW VIEWING: NEW PAPERS ▾

<input type="button" value="Submit File"/>		Online Grading Report Edit assignment settings Email non-submitters						
<input type="checkbox"/>	AUTHOR	TITLE	SIMILARITY	GRADE	RESPONSE	FILE	PAPER ID	DATE
<input type="checkbox"/>	Ahmed Zakwan	ABSTRACT	0%	--	--		2024921633	28-Feb-2023
<input type="checkbox"/>	Ahmed Zakwan	CHAPTER 5	0%	--	--		2024931455	28-Feb-2023
<input type="checkbox"/>	Ahmed Zakwan	CHAPTER 6	0%	--	--		2024931916	28-Feb-2023
<input type="checkbox"/>	Ahmed Zakwan	CHAPTER 1	1%	--	--		2024922606	28-Feb-2023
<input type="checkbox"/>	Ahmed Zakwan	CHAPTER 4	7%	--	--		2024929688	28-Feb-2023
<input type="checkbox"/>	Ahmed Zakwan	CHAPTER 3	9%	--	--		2024924109	28-Feb-2023
<input type="checkbox"/>	Ahmed Zakwan	ALL THESIS	10%	--	--		2024942728	28-Feb-2023
<input type="checkbox"/>	Ahmed Zakwan	CHAPTER 2	11%	--	--		2024923703	28-Feb-2023